frontiers in
MOLECULAR NEUROSCIENCE

ORIGINAL RESEARCH ARTICLE
published: 07 July 2009
doi: 10.3389/neuro.02.003.2009

Kv4 channels underlie the subthreshold-operating A-type K+-current in nociceptive dorsal root ganglion neurons

Thanawath Ratanadilok Na Phuket and Manuel Covarrubias*

Department of Pathology, Anatomy, and Cell Biology, Jefferson Medical College of Thomas Jefferson University, Philadelphia, PA, USA

Edited by:
Bernard Attali, Tel Aviv University, Israel

Reviewed by:
Florian Lesage, IPMC CNRS, France
Jeanne M. Nerbonne, Washington University School of Medicine, USA
James S. Trimmer, University of California, USA

***Correspondence:**
Manuel Covarrubias, Department of Pathology, Anatomy, and Cell Biology, Jefferson Medical College of Thomas Jefferson University, 1020 Locust Street, JAH 245, Philadelphia, PA 19107, USA.
e-mail: manuel.covarrubias@jefferson.edu

The dorsal root ganglion (DRG) contains heterogeneous populations of sensory neurons including primary nociceptive neurons and C-fibers implicated in pain signaling. Recent studies have demonstrated DRG hyperexcitability associated with downregulation of A-type K^+ channels; however, the molecular correlate of the corresponding A-type K^+ current (I_A) has remained hypothetical. Kv4 channels may underlie the I_A in DRG neurons. We combined electrophysiology, molecular biology (Whole-Tissue and Single-Cell RT-PCR) and immunohistochemistry to investigate the molecular basis of the I_A in acutely dissociated DRG neurons from 7- to 8-day-old rats. Whole-cell recordings demonstrate a robust tetraethylammonium-resistant (20 mM) and 4-aminopyridine-sensitive (5 mM) I_A. Matching Kv4 channel properties, activation and inactivation of this I_A occur in the subthreshold range of membrane potentials and the rate of recovery from inactivation is rapid and voltage-dependent. Among Kv4 transcripts, the DRG expresses significant levels of Kv4.1 and Kv4.3 mRNAs. Also, single small-medium diameter DRG neurons (~30 μm) exhibit correlated frequent expression of mRNAs encoding Kv4.1 and Nav1.8, a known nociceptor marker. In contrast, the expressions of Kv1.4 and Kv4.2 mRNAs at the whole-tissue and single-cell levels are relatively low and infrequent. Kv4 protein expression in nociceptive DRG neurons was confirmed by immunohistochemistry, which demonstrates colocalization of Kv4.3 and Nav1.8, and negligible expression of Kv4.2. Furthermore, specific dominant-negative suppression and overexpression strategies confirmed the contribution of Kv4 channels to I_A in DRG neurons. Contrasting the expression patterns of Kv4 channels in the central and peripheral nervous systems, we discuss possible functional roles of these channels in primary sensory neurons.

Keywords: voltage-gated K^+ channels, nociceptive neurons, RT-PCR, nucleofection, dominant-negative suppression

INTRODUCTION

Voltage-gated potassium (Kv) channels are quintessential regulators of electrical excitability in the nervous system. Within the superfamily of Shaker-related Kv channels, four sub-families (Kv1, Kv2, Kv3, and Kv4) are present in the nervous system of diverse organisms in the animal kingdom (Gutman et al., 2003; Salkoff et al., 1992). Although these Kv channels can produce delayed-rectifier and transient "A-type" currents (I_{DR} and I_A, respectively), all members of the Kv4 subfamily (Kv4.1, Kv4.2, and Kv4.3) mediate I_A (Birnbaum et al., 2004; Jerng et al., 2004). Kv4 channels in the central nervous system (CNS) localize to the soma and dendrites and, therefore, are responsible for the somatodendritic A-type K^+ current (I_{SA}) (Hoffman et al., 1997; Sheng et al., 1992). In hippocampal CA1 neurons, for instance, Kv4 channels are primarily expressed in distal dendrites where they dampen back-propagating action potentials and plateau potentials (Cai et al., 2004; Johnston et al., 2003). Depending on the frequency of repetitive spike firing Kv4 channels can also regulate the interspike interval (slow repetitive firing) and the duration of the action potential (fast repetitive firing) in CNS neurons (Khaliq and Bean, 2008; Kim et al., 2005; Song et al., 1998). In contrast, the functions and molecular correlates of I_A in the peripheral nervous system (PNS) are, in general, poorly understood. An important exception is the superior cervical sympathetic ganglion (SCG), where Kv4 subunits are the primary molecular correlate of the I_A (Malin and Nerbonne, 2000, 2001). Multiple studies have characterized voltage-dependent K^+ currents of dorsal root ganglion (DRG) neurons (Everill et al., 1998; Gold et al., 1996; Kostyuk et al., 1981; Safronov et al., 1996; Winkelman et al., 2005); and different groups have separately examined the relationship between nerve injury and I_A magnitude or the expression of Kv4 channels (Abdulla and Smith, 2001; Chien et al., 2007; Kim et al., 2002; Rasband et al., 2001; Tan et al., 2006). Kim et al. (2002) first showed that the lumbar DRG from adult rats expresses Kv4.1, Kv4.2 and Kv4.3 mRNAs, and that nerve injury selectively downregulates Kv4.2 and Kv4.3. More recently, Chien et al. (2007) employed quantitative immunohistochemistry in a neuropathic pain model to show an inverse link between mechanical hypersensitivity and the expressions of Kv3.4 and Kv4.3 in lumbar nociceptive DRG neurons from adult rats. In light of this evidence, it is reasonable to assume that Kv4 channels may underlie I_A in nociceptive DRG neurons. Testing this hypothesis more directly and systematically is a prerequisite toward understanding the mechanisms underlying nociception and pain plasticity.

The DRG contains a heterogeneous population of primary sensory neurons that are responsible for relaying peripheral sensory information to the CNS (Scott, 1992). Among various sensory

functions, the C- and Aδ-fibers associated with small-medium diameter sensory neurons serve nociceptive function and play an important role in inflammatory and neuropathic pain signaling (Scott, 1992). To probe the putative contribution of Kv4 channels to the I_A in these nociceptive DRG neurons (~30 μm) from newborn rats (7- to 8-day post-partum), we implemented a multipronged approach based on electrophysiological, molecular, and immunohistochemical techniques. At the mRNA and protein levels, the results demonstrate a prominent expression of Kv4.1 and Kv4.3 isoforms, which most likely underlie the subthreshold-operating I_A in DRG neurons from neonate rats. Accordingly, a specific dominant-negative strategy confirmed that Kv4 proteins are the molecular correlates of the DRG I_A. The primary expression of Kv4.1 and Kv4.3 channels in this system is significant because it differs sharply from the dominant and widespread expression of Kv4.2 and Kv4.3 channels in the CNS.

MATERIALS AND METHODS

ISOLATION OF DRG NEURONS

Sprague-Dawley rats (Taconic, Germantown, NY, USA) were treated according to the IACUC guidelines of Thomas Jefferson University. Time-pregnant female rats were delivered and maintained at the Thomas Jefferson University Animal Facility 1 week prior to birth of pups. For all experimental procedures reported here, we used 7- to 8-day-old pups. Before dissection, the pups were anesthetized using isoflurane and sacrificed by decapitation. The DRG tissue was dissected out from all accessible levels, trimmed of its peripheral nerve, and placed into Hank's Buffered Saline Solution (HBSS) containing 10 mM HEPES. Whole-tissue samples used for immunofluorescence were collected and preserved in Tissue-Tek OCT media (Electron Microscopy Science, Hatfield, PA, USA). Dissociation of individual DRG neurons was accomplished by two separate 30-min rounds of enzymatic treatment at 37°C. Following two washes with HBSS containing 10 mM HEPES, the first and second rounds involved incubations with 1.5 mg/mL of collagenase (Sigma, St. Louis, MO, USA) and 1 mg/mL trypsin (Sigma, St. Louis, MO, USA), respectively. The DRG neurons were placed into Neuronal Growth Media (NGM; see below) and dissociated by carefully triturating with a fire polished Pasteur pipette for approximately 15 times. Individual DRG neurons were then allowed to settle onto lysine (Sigma, St. Louis, MO, USA) coated cover slips for approximately 1 h prior to whole-cell recording. Electrophysiological recordings were performed within 72 h after harvesting.

ANTIBODIES

The monoclonal mouse anti-Kv4.2 and Kv4.3 antibodies (stocks at 1 mg/mL; 1:100 dilutions) were obtained from the UC Davis/NINDS/NIMH NeuroMab Facility (supported by NIH grant U24NS050606 and maintained by the Department of Pharmacology, School of Medicine, University of California, Davis, CA, USA). Several recent studies have characterized these antibodies (Burkhalter et al., 2006; Chien et al., 2007; Huang et al., 2005, 2006). The polyclonal rabbit anti-Nav1.8 antibody (Sigma, St. Louis, MO, USA) targeting the C-terminus of the channel was used as a nociceptive neuron marker (1:100 dilutions, as indicated by the manufacturer). Secondary antibodies (1:400 dilution) used for immunofluorescence were donkey anti-rabbit Alexa Fluor 488-conjugated and goat-anti-mouse Alexa Fluor 546-conjugated (Invitrogen, Carlsbad, CA, USA) or goat anti-rabbit Cy2-conjugated (Jackson ImmunoResearch Labs, Inc., West Grove, PA, USA). Nonspecific binding of secondary antibodies was tested by processing the samples in the absence of primary antibodies. Under these conditions, these assays revealed no immunofluorescence (data not shown).

IMMUNOHISTOCHEMISTRY

Ten micrometer fresh frozen tissue sections were prepared on a Shandon Cryotome (Thermo Scientific Inc., Waltham, MA, USA) and directly mounted onto glass slides. DRG tissue sections were fixed in 4% paraformaldehyde and blocked in Phosphate Buffered Solution (PBS) containing 0.1% Triton X-100 and 10% of appropriate serum (goat or donkey). Doubling the concentration of detergent resulted in similar staining patterns (data not shown). Primary antibodies were diluted (1:100) in blocking solution and incubated overnight. Secondary antibodies were diluted (1:400) in blocking solution and incubated for 1 h. Nuclear DNA was stained by either treating tissue sections with TO-PRO-3 (Invitrogen, Carlsbad, CA, USA) for 1 h and mounting slides in ProLong Gold Antifade reagent (Invitrogen, Carlsbad, CA, USA) or directly mounting slides in ProLong Gold Antifade reagent containing DAPI (Invitrogen, Carlsbad, CA, USA). Images were captured using a scanning confocal microscope (Zeiss LSM 510 META-UV) at Kimmel Cancer Center Bioimaging Facility (Thomas Jefferson University, Philadelphia, PA, USA) and images were acquired using the AxioVision v4.6 software (Carl Zeiss, Inc, Thornwood, NY, USA). The co-localization of Kv4.3 in nociceptive neurons (Nav1.8-positive) was examined in double labeling experiments (**Figure 5**).

WHOLE-TISSUE AND SINGLE-CELL RT-PCR

Whole-tissue DRG tissue (two to three ganglia of various spinal levels) was used to purify total RNA by the RNAqueos-4PCR Kit (Ambion, Inc., Austin, TX, USA). Genomic DNA contamination was eliminated by a 30-min DNase treatment. Extracted RNA was used to generate cDNA and subsequently for conventional RT-PCR and qRT-PCR. cDNA was synthesized from 300 ng of purified total RNA, 160 ng random primers, 10 ng oligo$(dT)_{12–18}$, 0.5 mM dNTPs, 10 mM DTT, 2 U RNase inhibitor, and 400 U Superscript II reverse transcriptase (Invitrogen, Carlsbad, CA, USA). Synthesis was performed by incubating at 25°C for 10 min, 42°C for 50 min, and 70°C for 15 min. Reactions were run in the presence and absence of reverse transcriptase (negative control). Conventional PCR was used to validate PCR primers and screen transcript expression of various genes. PCR reactions (20 μL) were performed using 1 μL of cDNA product, 0.5 mM gene specific primers (Table 1 in Supplementary Material), and HotStarTaq Plus Master Mix (Qiagen Inc., Valencia, CA, USA). Hot start reactions were initiated by a 5-min incubation at 95°C and amplifications were performed utilizing 35 cycles of 94°C for 30 s, 50°C for 30 s, and 72°C for 1 min. Transcript expression was detected using 5 μl of PCR product on a 2% agarose gel.

To determine the relative quantities of specific mRNAs by qRT-PCR, we used the Mx2005P QPCR System (Stratagene, La Jolla, CA, USA). A typical reaction consisted of diluted cDNA (1:5), 150 nM primers, and Brilliant II QPCR Master Mix. For calibration, measurements were performed in 96-well plates with serial dilutions (10–10^6 copies) of known templates (gel extracted

PCR products of known concentrations determined spectrophotometrically at 260 nm). All measurements were done in duplicates or triplicates, and sample variability was reduced by normalization using ROX as the internal standard. C_T values obtained from the amplification curves were then plotted against copy number in a semi-log format. The best-fit linear regression yielded the efficiency of the reaction (slope = −3.3 to −3.5) and the correlation coefficient (r^2 = 0.91–1). A slope = −3.31 represents a perfectly efficient reaction (Wong and Medrano, 2005). cDNA samples (1:5 dilutions) were ran together with serial dilutions to interpolate quantity of transcripts. All experimental sample curves were within range of serial dilutions. Negative controls (no RT and no template) were also sampled to rule out false positives. Results were normalized relative to β-actin expression. Measurements were performed on cDNA samples from a total of five different rat pups.

Single-cell RT-PCR was conducted as reported previously (Eberwine, 2001; Liss et al., 2001; Song et al., 1998). The patch-clamp recording pipette was used to harvest single neurons after whole-cell patch clamping. Negative pressure was applied to recover cellular contents and lift neurons (diameter ≈ 30 μm) off the cover slip. The pipette tip was crashed into a 0.2-mL PCR tube with 10 μL of RNase Inhibitor (Roche Applied Science, Indianapolis, IN, USA) containing H_2O and ~2 μL of contents were expelled by positive pressure. Samples were then frozen in methanol containing dry ice prior to cDNA synthesis. Single-stranded cDNA was synthesized using random primers (Invitrogen, Calsbad, CA, USA) and M-MLV RT (Fisher Scientific, Pittsburgh, PA, USA); and incubating at 42°C for 60 min. To verify the absence of contaminating mRNA, samples of bath solution were also reverse transcribed; and negative controls excluding RT were included. The reaction was terminated by heating the mixture to 92°C for 10 min. The single-cell cDNA synthesized from the reverse transcription step was subjected to nested PCR using a programmable thermal cycler (Applied Biosystems, Foster City, CA, USA), gene specific primers designed to be intron-flanking (0.5 μM, Table 1 in Supplementary Material), and 6.25 U Taq Polymerase (Roche Applied Science, Indianapolis, IN, USA). The first round of nested PCR contained 1 μL of the single-cell cDNA reaction (25 μL reaction); and the second round used 1 μL of the products from the first round and nested primers.

CONSTRUCTION AND EXPRESSION OF pEGFP-Kv4.2

The rat Kv4.2 sequence was PCR amplified from cDNA (pRC-CMV; gift from M. Sheng, Massachusetts Institute of Technology, Cambridge, MA, USA) using sense and anti-sense primers containing the Nhe I and Age I restriction sites, respectively (Table 1 in Supplementary Material). PCR products were gel purified (Qiagen, Valencia, CA, USA) and digested with Nhe I and Age I simultaneously. Digested PCR products were ligated into pEGFP-N1 digested with Nhe I and Age I (BD Biosciences Clontech, San Jose, CA, USA) plasmid that was treated with shrimp phosphatase (Roche Applied Science, Indianapolis, IN, USA) and gel extracted. To create a dominant-negative subunit, the W342F mutation was introduced into pEGFP-Kv4.2 using a site-directed mutagenesis strategy (QuickChange; Stratagene, La Jolla, CA, USA). All constructs were confirmed by automated sequencing at the Nucleic Acid Facility of the Kimmel Cancer Center (Thomas Jefferson University, Philadelphia, PA, USA).

The transfection of tsA-201 cells (gift from R. Horn, Thomas Jefferson University, Philadelphia, PA, USA) was accomplished using FuGENE 6 reagent (Roche Applied Science, Indianapolis, IN, USA) as recommended by the manufacturer. Cells were recorded 1–2 days post-transfection and under epi-fluorescence microscopy to confirm protein expression. Recording solutions used are indicated below.

NUCLEOFECTION OF DISSOCIATED DRG NEURONS

Acutely dissociated DRG neurons were transfected using the Amaxa Nucleofector II System (Amaxa Biosystems, Inc., Cologne, Germany). Either program G-013 or O-003 along with 3 μg of pEGFP-N1 (BD Biosciences Clontech, San Jose, CA, USA) or pEGFP-Kv4.2 and the Rat Neuron Nucleofector Kit were used to nucleofect approximately 2×10^6 cells. Immediately after pulsing, neurons were allowed to recover by adding DMEM media lacking Ca^{2+} or Mg^{2+} and incubated for 10 min at 37°C. Cells were then plated onto dishes containing lysine treated cover slips and NGM. Two-thirds of the media was replenished after ~4 h to remove dead/dying cells and any possible apoptotic factors. NGM media was supplemented with fresh NGF (100 ng/mL).

WHOLE-CELL ELECTROPHYSIOLOGY

Electrophysiological recordings from small-medium diameter DRG neurons (25–32 μm, 16–86 pF) were obtained in the whole-cell configuration of the patch-clamp method (Hamill et al., 1981) at room temperature (23.6 ± 0.4°C). Sylgard-coated (Dow Corning, Midland, MI, USA) patch electrodes were pulled with a PIP5 micropipette puller (HEKA, Southboro, MA, USA). All recordings were performed using thick-walled patch glass (Sutter Instruments Co., Novato, CA, USA), and were fashioned to have a tip resistance of ~1–3 MΩ. Signals were amplified by an Axopatch 200B amplifier (Axon Instruments Inc., Burlington, CA, USA), filtered at 2 kHz, digitized at 10 kHz, and stored in a computer using pClamp software v8.x (Axon Instruments Inc., Burlington, CA, USA). Data were analyzed from recordings with series resistance of less than 5 MΩ and with 75–95% compensation to minimize offsets due to large voltage-clamp errors. Liquid junction potentials were calculated and corrected off-line.

RECORDING SOLUTIONS AND MEDIA

Prior to use, all solutions and media were filtered with a 0.2 μm filter. NGM: Leibovitz L-15 Media, 10% fetal bovine serum, 2 mM L-glutamine, 24 mM $NaHCO_3$, 38 mM glucose, 2% penicillin-streptomycin, 50 ng/mL nerve growth factor (NGF) (Sigma, St. Louis, MO, USA). To record neuronal K^+ currents under voltage-clamp conditions, bath solution contained (in mM): 110 choline, 5 KCl, 1 $MgCl_2$, 2 $CaCl_2$, 10 HEPES, 20 tetraethylammonium (TEA), pH 7.4 with choline base. TEA was added to the bath solution to remove TEA-sensitive K^+ currents. When adding 5 mM 4-aminopyridine (4-AP) to the bath solution, the concentration of choline was decreased to 105 mM. The patch pipette solution contained (in mM): 120 KCl, 2.5 $MgCl_2$, 1 EGTA, 10 HEPES, 2 MgATP, 0.3 LiGTP, pH 7.3 with NaOH. To record from mammalian tsA-201 cells, the bath solution contained (in mM): 150 NaCl, 2 KCl, 1 $MgCl_2$, 1.5 $CaCl_2$, 10 HEPES, pH 7.4 with NaOH; and the following pipette solution: 120 KF, 2 $MgCl_2$, 1 $CaCl_2$, 11 EGTA, 10 HEPES, pH 7.2 with KOH. All chemicals were acquired from Invitrogen (Carlsbad,

CA, USA), Fisher Scientific (Pittsburgh, PA, USA) or Sigma Aldrich (St Louis, MO, USA).

DATA ACQUISITION AND ANALYSIS

A computer interfaced to a 16-bit A/D converter (Digidata 1320A using Clampex 8.x; Axon Instruments, Foster City, CA, USA) controlled the voltage-clamp protocols and data acquisition. Data analysis was conducted in Clampfit 9.x (Axon Instruments) and SigmaPlot 9.x (SPSS Inc.). The peak chord conductance (G_p) was calculated as follows:

$$G_p = I_p/(V_c - V_r)$$

I_p is the peak outward current, V_c is command voltage and V_r is the estimated reversal potential (−80 mV); and the resulting G_p–V relations were described assuming a fourth-order Boltzmann function:

$$G_p(V) = G_{pmax}\,[1/(1 + \exp((V_a - V_c)/k))]^4$$

G_{pmax} is the maximal peak conductance, k is the slope factor, and V_a is the activation mid-point voltage of a single subunit. The displayed G_p–V relations are normalized to the estimated G_{pmax} (G_p/G_{pmax}). The mid-point voltages of the G_p–V relations ($V_{1/2}$) were calculated from the following equation:

$$V_{1/2} = [V_a + (k \times 1.665)]$$

Steady-state inactivation curves were described assuming a first-order Boltzmann function; and the kinetics of macroscopic inactivation was described assuming the sum of two exponential terms plus a constant (Jerng and Covarrubias, 1997). All results throughout the manuscript were expressed as mean ± S.E.M. The one-way ANOVA test was applied to evaluate differences between data samples (Origin 7.5, OriginLab, Northhampton, MA, USA); and the Tukey multiple comparison test to evaluate multiple samples. The χ^2 test of independence (predicted frequencies > 5), the Fisher's exact test (predicted frequencies < 5)[1], and linkage analysis (Mendel 8.0)[2] were applied to test for correlations (**Figure 6**; **Table 2**, respectively).

RESULTS

ISOLATION AND CHARACTERIZATION OF A SUBTHRESHOLD-OPERATING A-TYPE K^+ CURRENT IN DRG NEURONS

We conducted whole-cell patch-clamp measurements to ask whether the electrophysiological properties of the I_A in small-medium diameter nociceptive DRG neurons (~30 μm, ~45 pF) are consistent with the expression of Kv4 channels. These channels are characteristically resistant to TEA (Amarillo et al., 2008; Birnbaum et al., 2004; Jerng and Covarrubias, 1997, 2004; Pak et al., 1991). Therefore, external TEA (20 mM) was present at all times to eliminate TEA-sensitive Kv channels (see Materials and Methods). In addition, by exploiting the distinct voltage dependence of inactivation of Kv4 channels, we employed voltage-clamp protocols to isolate the I_A (**Figure 1**). To measure the total K^+ current (I_K), neurons were held at −65 mV, and a 1-s conditioning pulse to −100 mV was delivered prior to 500-ms step depolarizations that typically activate Kv channels. The conditioning pulse permits ~90% recovery of the total I_A that inactivated at −65 mV. Then, the I_A was isolated from I_K by a depolarizing 1-s conditioning prepulse to −30 mV. This depolarization is sufficient to inactivate the I_A and, therefore, the remaining outward current evoked by subsequent step depolarizations is mostly comprised of a TEA-resistant delayed rectifying current (I_{DR}). I_A was finally revealed from the off-line subtraction of I_{DR} from I_K (**Figure 1**). About two-thirds the recorded neurons (30/46) exhibited a relatively fast I_A component that inactivates ≥80% in 500 ms and accounts for 87 ± 1% of the total peak I_K (range = 75–100%). After subtraction, the resulting currents of the remaining neurons displayed mostly slow-inactivating I_{DR} and small non-inactivating I_{DR} (data not shown). For further characterization, we focused on the population of neurons expressing relatively high levels of I_A. The absolute I_A ranges between 2.2 and 16.5 nA, and the mean I_A density is 275 ± 34 pA/pF (at +30 mV, n = 30).

The peak conductance–voltage relationship (G_p-V curve) of I_A shows detectable activation between −50 and −60 mV, and was well described by a 4th-order Boltzmann function with the following best-fit parameters: $V_{1/2}$ = −30 ± 10 mV and k = 16 ± 3.5 mV (n = 5) (**Figure 2A**; Table 1 in Supplementary Material). The voltage-dependence of steady-state inactivation was measured as the fraction of available peak current after 5-s pre-pulses to various membrane potentials (**Figures 2A,B**). The resulting steady-state inactivation curve was well described by a Boltzmann function with the following best-fit parameters: $V_{1/2}$ = −88 ± 4.8 mV and k = 7.8 ± 3.9 mV (n = 6). As expected, the voltage-independent fraction of the total current remaining at steady-state (0.08 ± 0.03) is very similar to the fraction of non-I_A resistant to the −30 mV conditioning pulse (**Figure 1B**). The sum of two exponential terms was necessary to describe the development of macroscopic inactivation at different membrane potentials between −20 and +60 mV (data not shown); and the resulting time constants exhibit weak voltage dependence (**Figure 3A**). The relative weights of the two components are equal at negative voltages, and the slow component is dominant at more positive voltages (**Figure 3B**). At +50 mV, τ_{fast} = 51 ± 24 ms (23%) and τ_{slow} = 270 ± 115 ms (61%, n = 12); and the extrapolated relative weight of an apparent sustained level of the I_A is 16.3 ± 2.9%.

Inactivation from closed states and rapid recovery from inactivation at hyperpolarized membrane potentials are hallmarks of Kv4 channels (Dougherty et al., 2008; Kaulin et al., 2008). In contrast, Kv1.4 channels (which may also contribute to I_A) exhibit recovery from inactivation that is 50–100 times slower (Petersen and Nerbonne, 1999). To investigate the recovery from inactivation of the I_A in DRG neurons, a 1-s step to −70 mV was delivered to induce substantial closed-state inactivation (>50%). This step was preceded by a 500-ms conditioning pulse to −100 mV to insure maximal availability of I_A before the recovery sequence. After the inactivating pulse, the membrane potential was stepped to the chosen recovery voltage (−100 or −120 mV) for increasing periods of time (Δt = 20 ms) before applying a standard test pulse (+50 mV, 100 ms). For each cycle of this protocol, the total control current (I_0) was first evoked by a 100-ms step depolarization to +50 mV after a conditioning pulse to −100 mV. The time course of recovery from closed-state inactivation is relatively fast

[1]http://udel.edu/~mcdonald/statintro.html

[2]http://www.genetics.ucla.edu/software/mendel

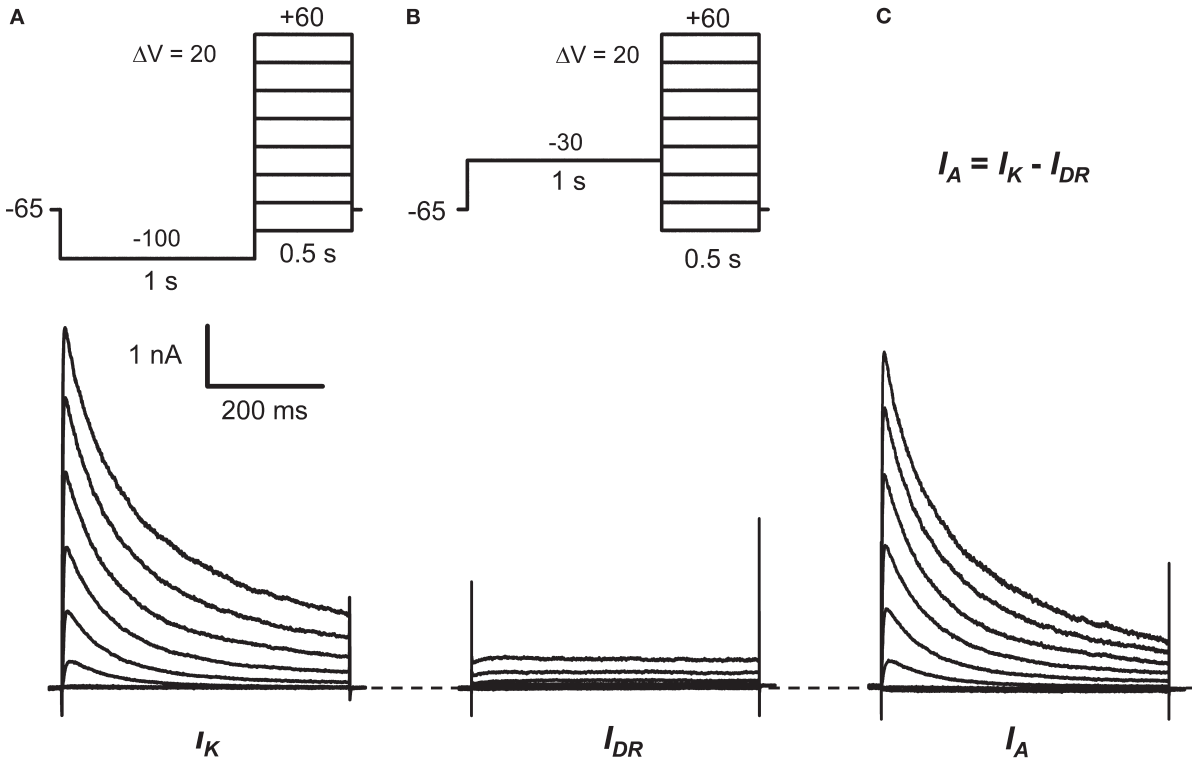

FIGURE 1 | Isolation of I_A in small DRG neurons. (A) Voltage-clamp protocol (top) to elicit the total K^+ current (I_K, bottom). From a holding voltage of –65 mV, a 1-s conditioning pulse at –100 mV precedes 500-ms step depolarizations delivered in 10-mV increments (for clarity, 20-mV increments are shown only). The start-to-start interval was 5 s. **(B)** Voltage-clamp protocol (top) to isolate the delayed-rectifier K^+ current (I_{DR}, bottom). The conditioning pulse at –30 mV inactivates the A-type K^+ current (I_A) **(Figure 2)**. **(C)** The subtraction of I_{DR} from I_K yielded I_A (bottom). These currents are from a DRG neuron (31 µm, 38 pF) exhibiting a dominant I_A (~90% I_A and ~10% I_{DR}; see Results).

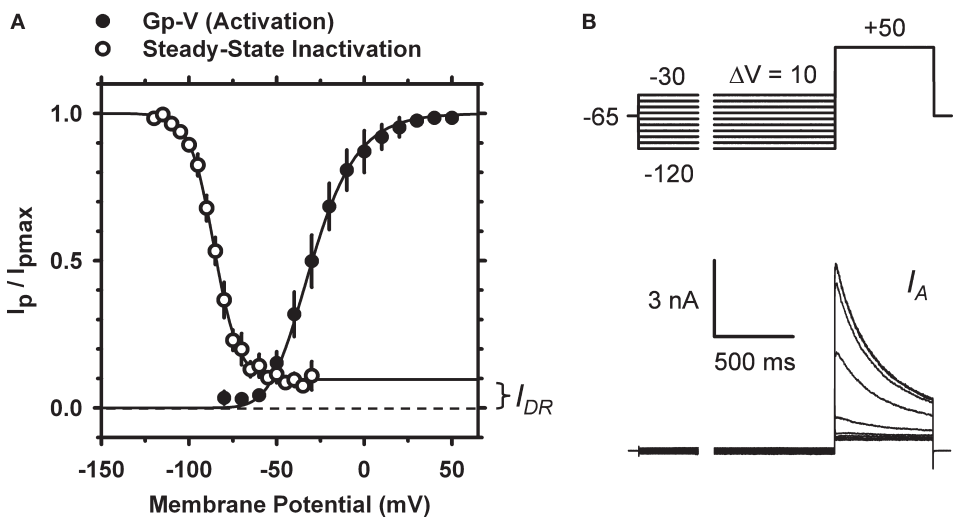

FIGURE 2 | Voltage-dependent activation and inactivation of I_A in small DRG neurons. (A) The peak conductance–voltage relation, (G_p–V relation, filled circles; n = 5) and the steady-state inactivation curve (empty circles; n = 6). A 4th-order Boltzmann function (*solid* line) describes the G_p–V relation with the following best-fit parameters: $V_{1/2}$ = –33 mV and k = 15 mV. A first-order Boltzmann function (*solid* line) best describes the steady-state inactivation curve with the following best-fit parameters: $V_{1/2}$ = –86 mV and k = 7 mV; the extrapolated non-inactivating component comprises 9.7% of the total current, and corresponds approximately to the level of the I_{DR} (**Figure 1**; see Results). In some instances, small error bars are obliterated by the data symbols. **(B)** Voltage-clamp protocol to determine the voltage dependence of I_A steady-state inactivation (top) and the resulting currents (bottom). The duration of the variable pre-pulse was 5 s (for display, a portion of the pre-pulse was blanked). These currents are from a DRG neuron (31 µm, 38 pF) exhibiting a dominant I_A (**Figure 1**; see Results).

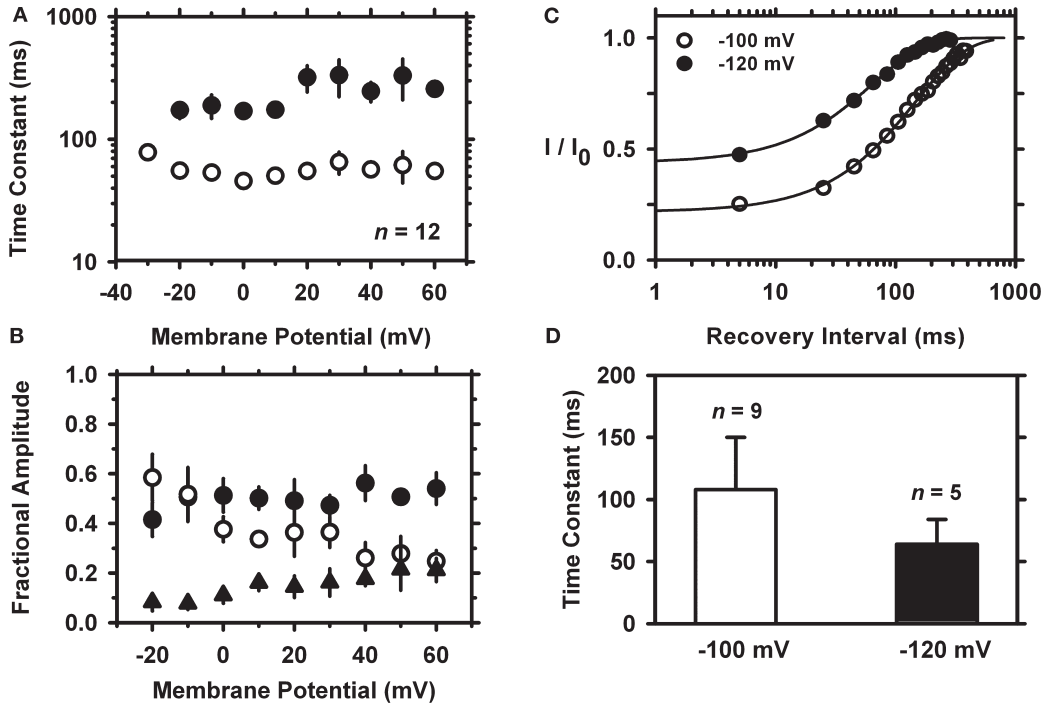

FIGURE 3 | Kinetics of macroscopic I_A inactivation (development and recovery) in small-medium diameter DRG neurons. (A) Voltage dependence of the fast (*empty* symbols) and slow (*solid* symbols) time constants for inactivation (n = 3–5). **(B)** Voltage dependence of the fractional amplitudes of the exponential terms (*solid* and *empty* circles) and the constant term (*solid* triangle). In some instances, small error bars are obliterated by the data symbols. **(C)** Normalized peak current (I/I_0) against the recovery interval at two membrane potentials. I_0 is the current evoked by the control pulse to +50 mV. The representative time courses at –100 (*empty* symbols) and –120 mV (*filled* symbols) are from two neurons. The *solid* lines are the best-fit exponential time courses. These neurons exhibited distinct levels of current resistant to inactivation. **(D)** Averaged time constants of recovery from inactivation at –100 and –120 mV. The means are significantly different at P = 0.048.

and approximately exponential, and the derived time constant exhibits significant voltage dependence (**Figure 3C**). At −100 and −120 mV, the time constants of the recovery from inactivation are 108 ± 42 ms (n = 9) and 63 ± 20 ms (n = 5), respectively (P = 0.048; **Figure 3D**). Overall, the voltage-dependent and kinetic properties of the TEA-resistant I_A in small-medium diameter nociceptive DRG neurons agree with the expression of Kv4 channels. In addition, the TEA-resistant I_A in these DRG neurons is reversibly inhibited by 5 mM 4-AP (65 ± 14%, n = 4), which is also characteristic of the subthreshold-operating I_A and Kv4 channels (Birnbaum et al., 2004; Jackson and Bean, 2007; Jerng et al., 2004; Pak et al., 1991; Song et al., 1998) (data not shown).

Kv4 CHANNEL EXPRESSION IN DRG NEURONS AT THE WHOLE-TISSUE AND SINGLE-CELL LEVELS

To investigate the contribution of Kv4 channels to the DRG I_A more directly, we applied several complementary approaches at the transcript and protein levels. First, we investigated whether pore-forming and auxiliary subunits are detectable in whole DRG tissue, which includes neuronal and non-neuronal cells. A broad end-point RT-PCR screening detected transcripts encoding all Kv4 isoforms and several auxiliary β-subunits thought to contribute to the neuronal Kv4 channel complex (Figure 1 in Supplemental Material) (Covarrubias et al., 2008). Other Kv channels were also detected, including Kv1.4, Kv1.5, Kv3.4, and Kvβ subunits that may confer an I_A phenotype to certain Kv1 channels (data not shown) (Bett and Rasmusson, 2008; Rettig et al., 1994). Then, we performed qRT-PCR to evaluate the relative amounts of Kv4 transcripts quantitatively (see Materials and Methods). The Kv4.1 and Kv4.3 isoforms are expressed at significantly greater levels than Kv4.2; and Kv4.1 is also expressed at a significantly greater level than Kv1.4 (**Figure 4**). The low expression of Kv4.2 mRNA in the DRG is noteworthy because this isoform is dominant in the CNS (Amarillo et al., 2008; Birnbaum et al., 2004; Jerng et al., 2004; Serodio and Rudy, 1998; Sheng et al., 1992; Shibata et al., 2000). Furthermore, the combined expression level of Kv4.1 and Kv4.3 is ~4-fold greater than that of Kv1.4 (**Figure 4**), which is also a putative component of A-type K^+ currents in the nervous system and the heart (Cooper et al., 1998; Nerbonne and Guo, 2002).

To more firmly support the contribution of Kv4 subunits to the channels that underlie the subthreshold-operating I_A in the DRG, we examined the expression of Kv4 proteins by immunohistochemical analysis (see Materials and Methods). The lack of reliable anti-Kv4.1 antibodies precluded the analysis of Kv4.1 expression at the protein level. Nevertheless, consistent with the qRT-PCR results, the neuronal immunostaining of Kv4.3 protein in the DRG is broad and robust (**Figure 5B**). As observed by others using anti-Kv channel antibodies in DRG and spinal neurons

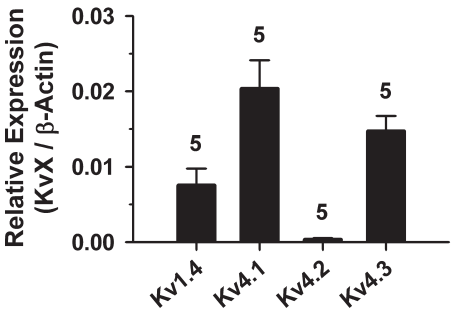

Tukey Test ($P < 0.01$)	Kv4.1	Kv4.2	Kv4.3
Kv1.4	S	NS	NS
Kv4.1	-	S	NS
Kv4.2	-	-	S

S = significant
NS = not significant

FIGURE 4 | qRT-PCR analysis of Kv4 channel expression in whole DRG. Bar graph comparing the relative expression of transcripts encoding Kv1.4, Kv4.1, Kv4.2 and Kv4.3. Absolute mRNA quantities (copy number) were determined from standard amplification plots and interpolation (see Materials and Methods). Kv channel expression is normalized to the expression of β-actin. *Inset*: Tukey multiple comparisons test. The samples were different from each other at $P = 0.0001$ (ANOVA) and the significance of paired comparisons at $P < 0.01$ is indicated in the grid.

(Binzen et al., 2006; Chien et al., 2007; Huang et al., 2005; Rasband et al., 2001; Vydyanathan et al., 2005), the anti-Kv4.3 immunostaining is partly cytosolic and possibly peri-nuclear. This pattern of expression suggests the presence of significant intracellular pools of Kv channel proteins in neuronal somata. Confirming the transcript analysis, the immunohistochemical analysis revealed little to no expression of Kv4.2 protein (**Figure 5A**). The Nav1.8 channel is a marker of a subpopulation of nociceptive DRG neurons (Akopian et al., 1999; Amaya et al., 2000; Djouhri et al., 2003). Accordingly, the immunostaining of DRG neurons with anti-Nav1.8 antibodies is distinct (and partially cytosolic) but less broad when compared to the immunostaining of Kv4.3 protein (**Figure 5C**). Suggesting the co-localization of Nav1.8 and Kv4 channels in subpopulations of nociceptive DRG neurons, double-labeling experiments revealed limited overlapping expression of Nav1.8 and Kv4.3 proteins (**Figure 5D**). In all cases, satellite glial cells, the other major cellular component of the DRG tissue, exhibit no immunostaining (**Figure 5**).

The transcript and protein analyses at the whole-tissue level yielded a broad picture of candidate subunits in the native Kv4 channel complex of DRG neurons. However, the DRG includes a heterogeneous population of neurons with distinct physiological roles (Scott, 1992); and therefore, evaluating Kv4 channel expression at the single-cell level would provide a more discrete picture. Particularly, single-cell expression analysis allows an independent assessment of the correlated expression of Kv4 and Nav1.8 channels in a selected population of nociceptive neurons. Earlier reports have shown the expression of Kv4 transcripts at the single-cell level in the CNS (Liss et al., 2001; Song et al., 1998). Similarly, we combined electrophysiology and molecular biology methodologies to study single DRG neurons (see Materials and Methods). After achieving the whole-cell recording configuration, the cytosolic material of a neuron (diameter ~30 μm) was collected in the patch pipette and subjected to nested RT-PCR (see Materials and Methods). In the first round of screening, the β-actin transcript was detected in 89% of the neurons ($n = 57$); and further screening of these samples revealed at least one Kv4 channel transcript in 29% of the neurons (14/49; **Figure 6B**). Although the Kv4.1 transcript is observed most frequently (22%, 12/54), only ~6% of the neurons are positive for either Kv4.2 or Kv4.3 (3/50 and 3/54, respectively). Kv1.4 and Nav1.8 are found in 11% and 52% of the total neurons, respectively (**Figure 6B**). The specific transcript categories and the expression frequencies are strongly correlated ($P < 0.0001$; $n = 47$). A relatively large fraction of neurons expressing the Nav1.8 transcript (26/50) suggests a significant proportion of nociceptive neurons in the selected population. Thus, we re-screened the samples and applied linkage analysis to pairs to test whether Kv4 and Nav1.8 transcripts co-exist at the single-cell level (see Materials and Methods; **Table 2**). Whereas 11/26 Nav1.8-positive neurons were also Kv4 positive, only 2/24 Nav1.8-negative were Kv4-positive. Given the relatively large number of Nav1.8- and Kv4.1-expressing neurons (an example from a single neuron is shown in **Figure 6A**), the corresponding samples demonstrate the most reliable linkage analysis results. A positive correlation between the expression of these transcripts does not occur by chance ($P = 0.02$, $D' = 0.65$); and therefore, the co-expression of Kv4.1 and Nav1.8 channels in small-medium diameter nociceptive neurons is likely. Since the expression frequencies of Kv1.4, Kv4.2 and Kv4.3 are low in the selected population (**Figure 6B**) other paired correlations could not be interpreted reliably. Collectively, however, the results from the immunohistochemical and single-cell RT-PCR analyses are clearly consistent with the expression of two Kv4 isoforms (Kv4.1 and Kv4.3) in nociceptive neurons (Nav1.8-positive). Kv4 subunits are thus strong candidate components of the channel complex that underlies I_A in DRG neurons as suggested by the biophysical and pharmacological analyses of the whole-cell K^+ currents (**Figures 1–3**).

A Kv4-SPECIFIC DOMINANT-NEGATIVE SUBUNIT SUPPRESSES I_A DRAMATICALLY

If the Kv channels underlying I_A in nociceptive DRG neurons are composed of Kv4 subunits, the expression of exogenous Kv4.2 subunits should selectively modulate the expression and biophysical properties of the native I_A by specific tetramerization with endogenous Kv4 subunits (namely, Kv4.1 and Kv4.3). Thus, to test this hypothesis, we transfected mammalian tsA-201 cells and dissociated DRG neurons with the following constructs (see Materials and Methods): EGFP (mock control), Kv4.2-EGFP (wild-type), and Kv4.2DN-EGFP (DN, dominant-negative). The fluorescent EGFP moiety was fused at the C-terminus of the Kv4.2 subunits

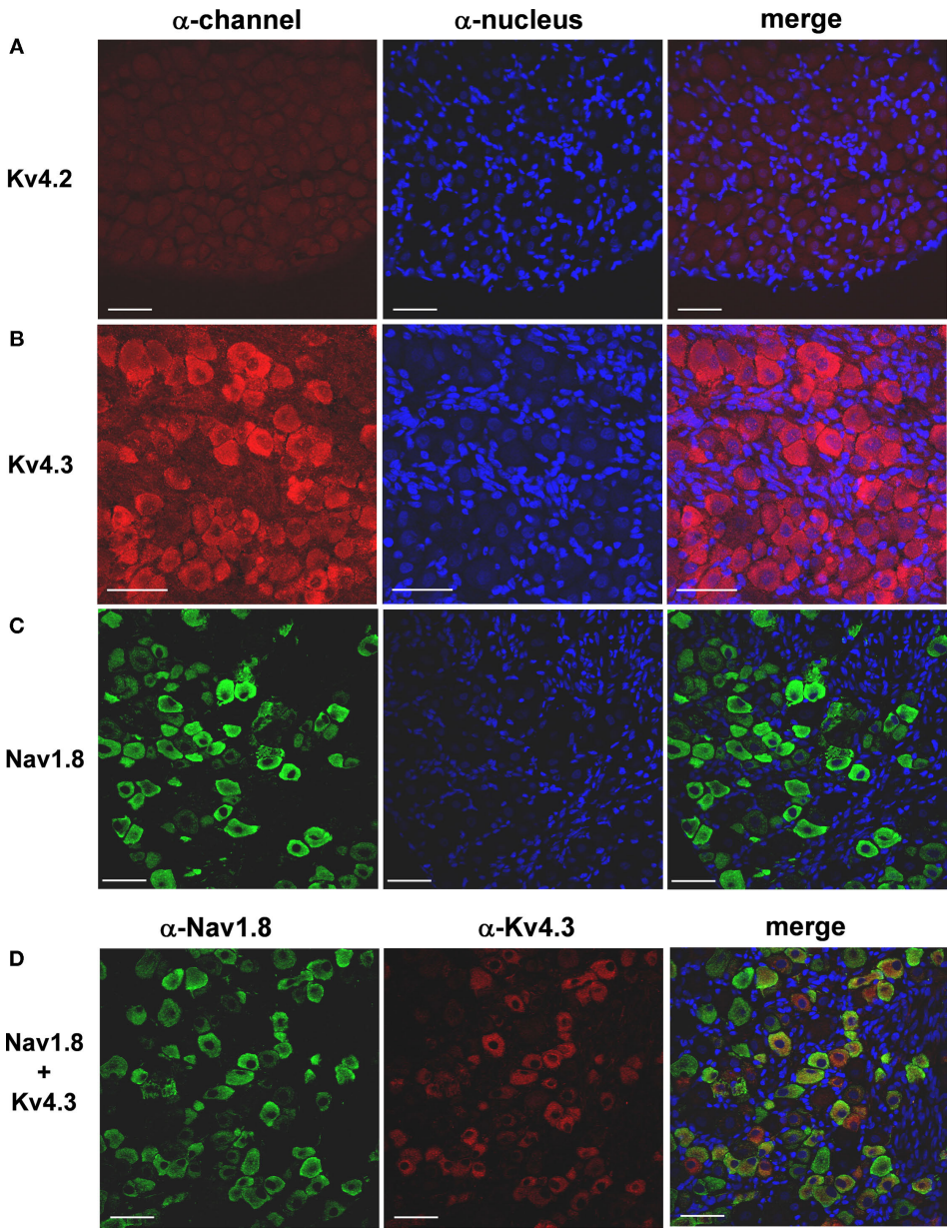

FIGURE 5 | Expression of Kv4.3 and Nav1.8 proteins in DRG neurons. Fresh frozen DRG sections (10 μm) were treated with specific antibodies against either Kv4 or Nav1.8 proteins. The expression was then evaluated by immunofluorescence and confocal microscopy (*left* column, α-channel; see Materials and Methods). The cell nuclei were stained with DAPI or TO-PRO-3 (α-nucleus, *middle* column). The merging of the images in the *left* and *middle* columns is shown on the *right* column. **(A)** The Kv4.2 protein does not express in the DRG. **(B)** The Kv4.3 protein is widely expressed in a heterogeneous population of DRG neurons. **(C)** The expression of the Nav1.8 protein is more restricted but limited to DRG neurons. The Nav1.8 protein is a marker of nociceptors (see Results). **(D)** Although several DRG neurons were found to express either Nav1.8 or Kv4.3 proteins exclusively, a sub-population of nociceptive neurons co-expresses Kv4.3 and Nav1.8. Similar results were obtained in experiments from two additional rats. Scale bar = 50 μm.

to permit visual detection of transfected cells. In mammalian tsA-201 cells, Kv4.2-EGFP induced typical Kv4.2 whole-cell currents exhibiting rapid activation and inactivation; and the voltage range of operation is similar to that of Kv4.2 channels lacking EGFP (Dougherty and Covarrubias, 2006; Dougherty et al., 2008; Kim et al., 2005) (**Figure 7**; data not shown). The dominant-negative effect of the Kv4.2DN-EGFP mutant was validated in tsA-201 cells co-transfected with Kv4.2-EGFP and Kv4.2DN-EGFP (**Figure 7**). The presence of at least one Kv4.2DN-EGFP subunit in the Kv4 channel tetramer should reduce the fraction of functional Kv4.2 channels in the cell. Expression of Kv4.2-EGFP alone induces transient currents that were often beyond the patch-clamp amplifier's range at depolarized voltages (**Figure 7A**). In contrast, co-expression of Kv4.2-EGFP and Kv4.2DN-EGFP results in a profound suppression of the I_A. At +10 mV, the current density is suppressed by 66% (**Figure 7B**).

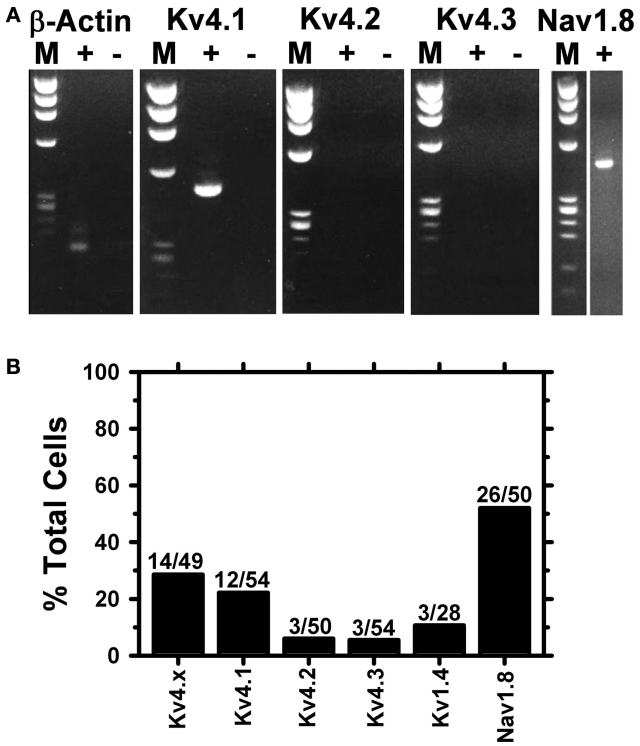

FIGURE 6 | Single-cell RT-PCR analysis from small DRG neurons. (A) The cellular content of a single DRG neuron was captured in the recording pipette after whole-cell recording. The recorded outward current exhibited a relatively slow I_A phenotype (not shown) similar to that observed from other small-medium diameter DRG neurons (**Figure 1**). Upon processing of the cellular content and amplification by nested RT-PCR (see Materials and Methods), the products were analyzed in a 2% agarose gel. The bands detected correspond to the predicted amplicons for β-actin, Kv4.1, and Nav1.8 (Table 1 in Supplementary Material). **(B)** Bar graph comparing the detection frequencies of various transcript categories in single-cell RT-PCR experiments. The first bar indicates that all three Kv4 transcripts were detected in 14/49 neurons. The χ^2 test of independence applied to the remaining bars revealed a statistically significant association between the transcript categories and the expression frequencies ($P < 0.0001$; $\chi^2 = 47$).

Since the Kv4.2-EGFP and Kv4.2DN-EGFP subunits behaved as expected in tsA-201 cells, we proceeded to express them in dissociated DRG neurons to specifically manipulate I_A properties (nucleofection; see Materials and Methods). Typically, neurons were examined 24–72 h post-nucleofection and only fluorescent neurons expressing the extrinsic proteins were included in the experiment. Although the endogenous Kv4.2 isoform expresses poorly in DRG neurons from newborn rats (**Figures 4–6**), extrinsic Kv4.2 subunits can form homomultimeric and novel heteromultimeric channels in these cells. The expression of exogenous Kv4.2-EGFP subunits in this experiment exploits interactions mediating highly specific heterotetramerization among members of the same Kv channel subfamily only (Covarrubias et al., 1991). Thus, suppression of the native I_A by expressing Kv4.2DN-EGFP subunits would involve the formation of novel non-functional Kv4 channels resulting from the interaction of at least one Kv4.2DN-EGFP subunit with native Kv4.1 and/or Kv4.3 subunits in the neuron. Although the I_A density of control neurons (mock-nucleofected with the EGFP plasmid only) remains stable during the 24–72 h post-nucleofection, over-expression of Kv4.2-EGFP significantly enhances the neurons' I_A density (**Figures 8A,B**). Moreover, consistent with the over-expression of rapidly inactivating Kv4.2 channels and the formation of novel heteromultimeric Kv4 channels, the larger I_A exhibits an intermediate development of macroscopic inactivation (**Figure 8B**). At +20 mV, the time constants of inactivation of over-expressed I_A are 26.5 ± 3.8 and 142 ± 11 ms, and the corresponding relative weights are 35 ± 5 and 57 ± 6% ($n = 7$). Relative to the kinetics of I_A inactivation in control DRG neurons (**Figure 3**) and tsA-201 cells transfected with Kv4.2-EGFP at +20 mV (**Figure 7**), these time constants are intermediate and significantly different ($P < 0.049$). In sharp contrast, Kv4.2DN-EGFP expression suppresses I_A dramatically, especially 48–72 h post-nucleofection (**Figure 8C**). At +20 mV, over-expression and suppression resulted in ~2.7-fold increase and ~3.5-fold reduction in the peak I_A density, respectively (**Figure 8D**). As expected, these effects are specific because the expression of the Kv4.2-EGFP and Kv4.2DN-EGFP subunits influences the I_A component but has no effect on the residual I_{DR} component (**Figure 8E**). These results are compelling evidence for a significant contribution of Kv4 subunits to the Kv channels that underlie I_A in DRG neurons.

DISCUSSION

This study is a comprehensive investigation of the contribution of Kv4 channels to the subthreshold-operating I_A in DRG neurons. A multipronged approach based on electrophysiological, molecular and biochemical analyses demonstrates that Kv4 subunits (mainly Kv4.1 and Kv4.3) are highly expressed in DRG neurons from 7- to 8-day-old rats, and most likely underlie I_A in this system.

FUNCTIONAL EVIDENCE OF Kv4 CHANNELS IN NOCICEPTIVE DRG NEURONS

In agreement with previous electrophysiological studies (Everill et al., 1998; Gold et al., 1996; Kostyuk et al., 1981; Safronov et al., 1996; Winkelman et al., 2005), whole-cell patch-clamp recordings from small-medium diameter nociceptive DRG neurons revealed an I_A with voltage-dependent, kinetic and pharmacological properties characteristic of subthreshold-operating neuronal Kv4 channels (Jerng et al., 2004) (**Figures 1–3**; **Table 1**). The functional properties of neuronal Kv4 channels are tailored to impact action potential firing, slow repetitive firing and the overall membrane excitability (Khaliq and Bean, 2008; Kim et al., 2005; Song et al., 1998; Yuan et al., 2005). In particular, the fast voltage-dependent recovery from inactivation of the I_A (**Figure 3**) supports the presence of Kv4 channels in DRG neurons (Amarillo et al., 2008; Dougherty et al., 2008; Jerng et al., 2004; Kaulin et al., 2008). This feature allows quick re-priming of Kv4 channels whenever the membrane potential is hyperpolarized. As a result, activation of these channels by a subsequent subthreshold depolarization can suppress or delay action potential firing. In sharp contrast, I_A resulting from Kv1.4 channel expression exhibits a time constant of recovery from inactivation >50-fold slower than that of Kv4 channels (Petersen and Nerbonne, 1999). Although Kv1.4 channels have been found in small diameter DRG neurons (**Figures 4 and 6**) (Binzen et al., 2006; Rasband et al., 2001), their functional role is probably different from that of Kv4 channels. Slow recovery from inactivation can cause cumulative inactivation in Kv1.4 channels

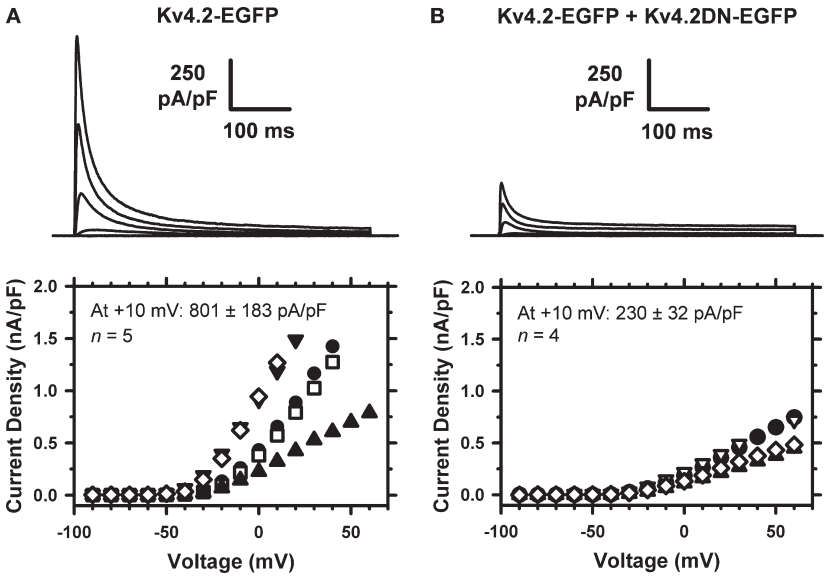

FIGURE 7 | Dominant-negative suppression of Kv4.2 currents expressed in tsA-201 cells. The whole-cell peak current density was determined in cells expressing Kv4.2-EGFP only **(A)** or co-expressing Kv4.2-EGFP and Kv4.2DN-EGFP **(B)**. The voltage-clamp protocol typically consisted of step depolarizations from –90 to +60 in 10-mV increments. The holding voltage was –100 mV and the start-to-start interval was 5 s. The traces shown correspond to –40, –20, 0 and +20 mV. The corresponding *I–V* relations from individual cells are shown below the families of currents, and the average peak current density is displayed in the graphs. The difference between the means is significant at $P = 0.03$.

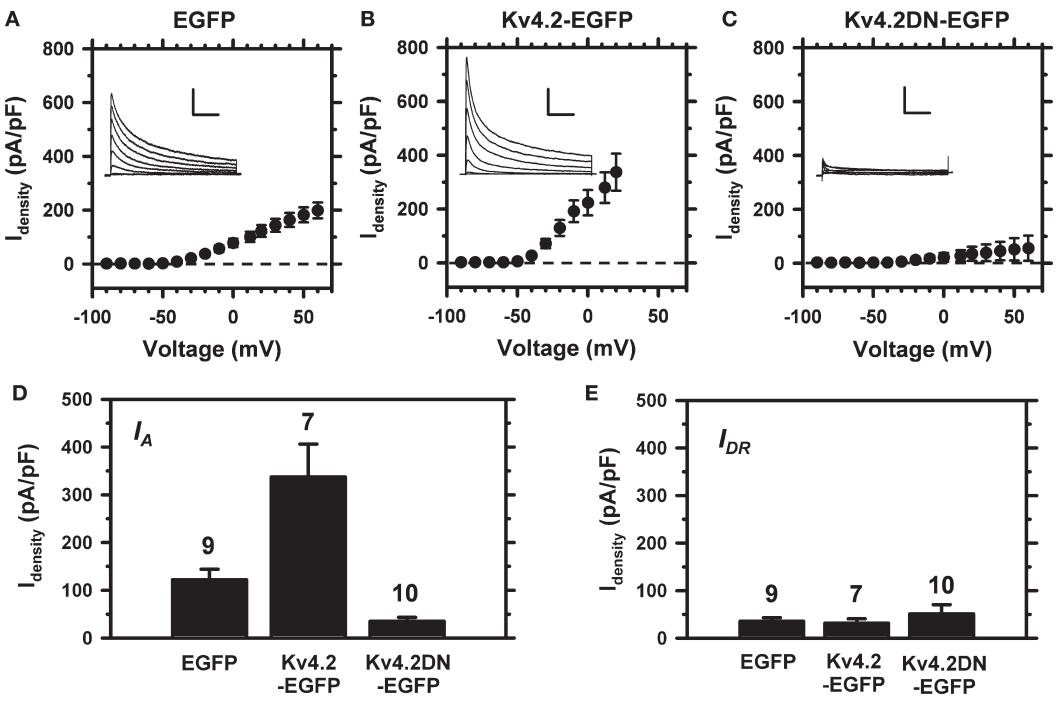

FIGURE 8 | Experimental manipulation of Kv4 channel expression in small-medium diameter DRG neurons. Neurons were nucleofected (see Materials and Methods) and I_A was isolated as shown in **Figure 1**. The peak current density from fluorescent DRG neurons was measured 24–72 h post-nucleofection. **(A)** I_A–*V* relation from DRG neurons expressing EGFP ($n = 9$). **(B)** I_A–*V* relation from DRG neurons expressing Kv4.2-EGFP ($n = 8$). **(C)** I_A–*V* relation from DRG neurons expressing Kv4.2DN-EGFP ($n = 10$). *Insets*: Representative I_A families of traces elicited by step depolarizations from –90 to +60 mV in 20-mV increments. Vertical and horizontal scale bars represent 3 nA and 100 ms, respectively. The holding voltage between pulse sequences was –65 mV. **(D)** Relative to the mock nucleofected neurons (EGFP), the differences between the I_A density means at +20 mV are statistically significant: EGFP vs. Kv4.2-WT ($P = 0.0051$), EGFP vs. Kv4.2DN-EGFP ($P = 0.0012$). **(E)** The I_{DR} isolated as shown in **Figure 1** is not affected by expressing EGFP or the Kv4.2 proteins.

Table 1 | Biophysical properties of the subthreshold-operating I_A in DRG neurons.

Property	Mean ± S.E.M	*n*
G_p–V RELATION		
$V_{1/2}$ (mV)	–33 ± 4.7	5
k (mV)	15 ± 1.4	
STEADY-STATE INACTIVATION		
$V_{1/2}$ (mV)	–88 ± 2	6
k (mV)	7.8 ± 1.6	
DEVELOPMENT OF INACTIVATION[a]		
τ_{FAST} (ms)	51 ± 7	12
W_{FAST} (%)	23 ± 3.2	
τ_{SLOW} (ms)	270 ± 33	
W_{SLOW} (%)	61 ± 3.7	
W_C (%)	16 ± 2.9	
RECOVERY FROM INACTIVATION[b]		
$\tau_{-100\ mV}$ (ms)	108 ± 14	9
$\tau_{-120\ mV}$ (ms)	63 ± 8.8	5

[a]*Parameters derived from a double exponential fit; measured at +50 mV. W_{FAST} W_{SLOW} and W_C are the relative weights of the exponential terms and constant term, respectively* ***(Figure 3)****.*

[b]*Time constants derived from an exponential fit of the time course of recovery from inactivation; measured at –100 and –120 mV. The difference between these time constants is statistically significant at P = 0.048* ***(Figure 3)****.*

during episodes of repetitive spike firing, which may then increase excitability of neurons in an activity-dependent manner (Engel et al., 1996; Roeper et al., 1997).

The relatively slow development of I_A macroscopic inactivation observed here (**Figures 1–3 and 8**) is similar to that previously reported for peripheral sensory neurons (Gold et al., 1996; Sculptoreanu et al., 2004; Vydyanathan et al., 2005; Winkelman et al., 2005). However, compared to the inactivation profile of the CNS I_A, it is significantly slower (Jerng et al., 2004). Slower inactivation could result from the co-assembly of Kv4 subunits and specific KChIP isoforms. For instance, KChIP4a eliminates fast inactivation of reconstituted and native Kv4 channels (Baranauskas, 2004; Holmqvist et al., 2002). Also, slow inactivation could be an intrinsic property of the Kv4 isoform expressed in DRG neurons. Among members of the Kv4 subfamily, Kv4.1 channels exhibit the slowest development of inactivation (Jerng et al., 2004); and the expression of the Kv4.1 subunit in small-medium diameter DRG neurons from newborn rats is exceptionally high (**Figures 4 and 6**; below). Slow inactivation of Kv4 channels may play an important physiological role by enhancing the I_A's ability to dampen excitability over extended periods. Future studies focusing on the auxiliary β-subunits in the DRG Kv4 channel complex may shed more light on these possibilities.

MOLECULAR EVIDENCE OF Kv4 SUBUNITS IN NOCICEPTIVE DRG NEURONS

Toward unveiling the molecular composition of I_A, we implemented a systematic approach to examine the expression of relevant subunits at the mRNA and protein levels in whole tissue and single-cell studies (**Figures 4–6**). The main results indicate that all putative components of the neuronal Kv4 channel complex are present in the DRG (Kv4 subunits, KChIPs, DPP6 and DPP10; Figure 1 in Supplemental Material); and that the Kv4.1 and Kv4.3 subunits are the dominant isoforms. Furthermore, the mRNA and immunohistochemical analyses showed co-expression of Kv4 and Nav1.8 channels at the whole-tissue and single-cell levels (**Figures 5 and 6**; **Table 2**), which favors the idea of Kv4 channels underlying the I_A in subpopulations of small-medium diameter nociceptive DRG neurons. Overall, this conclusion agrees with the results from earlier DRG studies that analyzed the expression of Kv4 mRNA and protein in adult rat models of neuropathic pain and suggested the contribution of Kv4 channels to the I_A and their role in pain plasticity (Chien et al., 2007; Kim et al., 2002). In addition, certain nociceptive DRG neurons display preferential binding of the isolectin glycoprotein (IB_4) and distinct electrical properties (Fang et al., 2006; Stucky and Lewin, 1999; Vydyanathan et al., 2005). Particularly, the density of 4-AP sensitive K^+ currents is higher in IB_4-positive neurons; and these neurons express larger TTX-resistant Na^+ currents (either Nav1.8 or Nav1.9 channels). Thus, the expression of Kv4 channels in a specific subpopulation of nociceptive IB_4-positive DRG neurons is an attractive possibility (Chien et al., 2007). The relatively low incidence of neurons expressing the Kv4.3 transcript at the single-cell level appears at odds with the results from whole-tissue qRT-PCR and immunohistochemistry, which detected significant expression of the Kv4.3 transcript and protein, respectively. This outcome may have resulted from the heterogeneous expression of Kv4.3 channels in DRG neurons and the cell selection criterion based on diameter (~30 μm) for the single-cell expression analysis. Kv1.4 channels may also contribute to a TEA-resistant I_A in a distinct population of small diameter nociceptive DRG neurons (Binzen et al., 2006; Rasband et al., 2001). Whether or not the expression patterns of Kv4 and Kv1.4 channels overlap in these neurons is, however, not known. The Kv3.4 protein is another potential molecular correlate of I_A in DRG neurons (Chien et al., 2007); however, its contribution to the TEA-resistant K^+ currents characterized here is unlikely because Kv3 channels are TEA-hypersensitive and activate at depolarized membrane potentials (Vega-Saenz et al., 1992).

Table 2 | Pairwise linkage analysis of single-cell expression[a].

Pairs	*P*-value	*D'*-value
Kv4.1–Kv4.2	0.155	0.555
Kv4.1–Kv4.3	0.159	0.555
Kv4.1–Nav1.8	0.0198	0.652
Kv4.2–Kv4.3	0.00760	0.644
Kv4.2–Nav1.8	1.00	0.304
Kv4.3–Nav1.8	0.609	–0.360

[a]*Pairwise statistical analysis of transcript co-expression using Mendel version 8.0 (Lange et al., 2005) (see Materials and Methods). Statistical significance ($P < 0.05$) for either positive-correlation ($1 > D' > 0$) or negative-correlation ($-1 < D' < 0$) was examined for Kv4 and Nav1.8 transcripts. Total sample size = 48. Since the number of Kv4.2- and Kv4.3-positive cells was very low in this sample* ***(Figure 6)****, the Kv4.2-Kv4.3 correlation cannot be interpreted.*

The expression of Kv4.1 in DRG neurons is noteworthy (Kim et al., 2002; Winkelman et al., 2005). While the Kv4.2 and Kv4.3 subunits are expressed throughout the brain and cerebellum of adult rats, the expression of the Kv4.1 subunit in the rat CNS is very low and discrete (Amarillo et al., 2008; Liss et al., 2001; Serodio and Rudy, 1998; Song et al., 1998). In contrast, our results demonstrate that the Kv4.1 and Kv4.3 subunits are broadly expressed in DRG neurons from newborn rats, whereas the Kv4.2 subunit is nearly absent in these cells (**Figures 4–7**). The functional expression of Kv4.1 channels may be more relevant in the PNS. However, the expression of Kv4.2 channels may be developmentally regulated in the DRG because previous studies suggest significant expression of all Kv4 transcripts in the DRG from adult rats, and a reduction in Kv4.2 and Kv4.3 expression in nerve injury models (Chien et al., 2007; Kim et al., 2002). Developmentally regulated expression of Kv4.2 and Kv4.3 subunits has been observed in spinal neurons (Huang et al., 2006).

Kv4 CHANNELS ARE THE MOLECULAR CORRELATES OF I_A IN DRG NEURONS

The electrophysiological and molecular analyses suggest the contribution of Kv4 subunits (at the transcript and protein levels) to I_A in small-medium diameter DRG neurons. A more definitive link between Kv4 subunits and the subthreshold-operating I_A emerged from the electrophysiological impact of expressing exogenous wild-type and mutant Kv4 subunits in DRG neurons. It has been established that Kv channel subunits only associate with members of the same subfamily (Covarrubias et al., 1991; Li et al., 1992). Thus, finding a profound suppression of the I_A upon expression of Kv4.2DN-EGFP, and I_A with intermediate kinetics of inactivation upon expression of Kv4.2-EGFP indicate the presence of endogenous Kv4 subunits that heterotetramerize with the recombinant Kv4 subunits. These results confirm that Kv4 channels are the molecular correlates of I_A in DRG neurons from newborn rats.

How do Kv4 channels underlying I_A regulate DRG neuron excitability? Further work beyond the scope of this study is necessary to answer this question. Nevertheless, we suggest that I_A impacts the regulation of spiking by subthreshold changes in the membrane potential (Khaliq and Bean, 2008; Korngreen et al., 2005). At a typical resting membrane potential of a neuron (e.g., −65 mV), I_A may have no impact on excitability because it undergoes steady-state inactivation. However, even a relatively brief hyperpolarization could help I_A quickly recover from inactivation and, consequently, influence timing (latency and interspike interval) and duration of an action potential resulting from a subsequent depolarizing stimulus. The hyperpolarization may result from a prolonged afterhyperpolarization, activation of background K^+ channels or inhibition of leak channels. Additionally, the activity of I_A may depend on the developmentally regulated composition of Kv4 tetramers and their association with accessory β-subunits, which could affect the biophysical and biochemical properties of the I_A.

ACKNOWLEDGMENT

This work was supported by NIH grants R01 NS032337 (MC) and T32 AA007463 (TRNP) and a Foerderer Pre-doctoral Fellowship (TRNP); and in part by a REA award from Thomas Jefferson University (MC). We thank Drs. C. Beck, K. Dougherty, J. Eberwine, R. Horn, Y. Kaulin and M. O'Leary for critical comments and insightful suggestions; and members of the Covarrubias lab for constructive feedback. In part, this work fulfilled a requirement toward the doctoral degree of TRNP in Molecular Cell Biology at Thomas Jefferson University.

SUPPLEMENTARY MATERIAL

The Supplementary Material for this article can be found online at http://www.frontiersin.org/molecularneuroscience/paper/10.3389/neuro.02/003.2009.

REFERENCES

Abdulla, F. A., and Smith, P. A. (2001). Axotomy- and autotomy-induced changes in Ca^{2+} and K^+ channel currents of rat dorsal root ganglion neurons. *J. Neurophysiol.* 85, 644–658.

Akopian, A. N., Souslova, V., England, S., Okuse, K., Ogata, N., Ure J., Smith, A., Kerr, B. J., McMahon, S. B., Boyce, S., Hill, R., Stanfa, L. C., Dickenson, A. H., and Wood, J. N. (1999). The tetrodotoxin-resistant sodium channel SNS has a specialized function in pain pathways. *Nat. Neurosci.* 2, 541–548.

Amarillo, Y., Santiago-Castillo, J. A., Dougherty, K., Maffie, J., Kwon, E., Covarrubias, M., and Rudy, B. (2008). Ternary Kv4.2 channels recapitulate voltage-dependent inactivation kinetics of A-type K^+ channels in cerebellar granule neurons. *J. Physiol.* 586, 2093–2106.

Amaya, F., Decosterd, I., Samad, T. A., Plumpton, C., Tate S., Mannion, R. J., Costigan, M., and Woolf, C. J. (2000). Diversity of expression of the sensory neuron-specific TTX-resistant voltage-gated sodium ion channels SNS and SNS2. *Mol. Cell Neurosci.* 15, 331–342.

Baranauskas, G. (2004). Cell-type-specific splicing of KChIP4 mRNA correlates with slower kinetics of A-type current. *Eur. J. Neurosci.* 20, 385–391.

Bett, G. C., and Rasmusson, R. L. (2008). Modification of K^+ channel-drug interactions by ancillary subunits. *J. Physiol.* 586, 929–950.

Binzen, U., Greffrath, W., Hennessy, S., Bausen, M., Saaler-Reinhardt, S., and Treede, R. D. (2006). Co-expression of the voltage-gated potassium channel Kv1.4 with transient receptor potential channels (TRPV1 and TRPV2) and the cannabinoid receptor CB1 in rat dorsal root ganglion neurons. *Neuroscience* 142, 527–539.

Birnbaum, S. G., Varga, A. W., Yuan, L. L., Anderson, A. E., Sweatt, J. D., and Schrader, L. A. (2004). Structure and function of Kv4-family transient potassium channels. *Physiol. Rev.* 84, 803–833.

Burkhalter, A., Gonchar, Y., Mellor, R. L., and Nerbonne, J. M. (2006). Differential expression of I_A channel subunits Kv4.2 and Kv4.3 in mouse visual cortical neurons and synapses. *J. Neurosci.* 26, 12274–12282.

Cai, X., Liang, C. W., Muralidharan, S., Kao, J. P., Tang, C. M., and Thompson, S. M. (2004). Unique roles of SK and Kv4.2 potassium channels in dendritic integration. *Neuron* 44, 351–364.

Chien, L. Y., Cheng, J. K., Chu, D., Cheng, C. F., and Tsaur, M. L. (2007). Reduced expression of A-type potassium channels in primary sensory neurons induces mechanical hypersensitivity. *J. Neurosci.* 27, 9855–9865.

Cooper, E. C., Milroy, A., Jan, Y. N., Jan, L. Y., and Lowenstein, D. H. (1998). Presynaptic localization of Kv1.4-containing A-type potassium channels near excitatory synapses in the hippocampus. *J. Neurosci.* 18, 965–974.

Covarrubias, M., Bhattacharji, A., Santiago-Castillo, J. A., Dougherty, K., Kaulin, Y. A., Na-Phuket, T. R., and Wang, G. (2008). The neuronal Kv4 channel complex. *Neurochem. Res.* 33, 1558–1567.

Covarrubias, M., Wei, A. A., and Salkoff, L. (1991). Shaker, Shal, Shab, and Shaw express independent K^+ current systems. *Neuron* 7, 763–773.

Djouhri, L., Fang, X., Okuse, K., Wood, J. N., Berry, C. M., and Lawson, S. N. (2003). The TTX-resistant sodium channel Nav1.8 (SNS/PN3): expression and correlation with membrane properties in rat nociceptive primary afferent neurons. *J. Physiol.* 550, 739–752.

Dougherty, K., and Covarrubias, M. (2006). A dipeptidyl aminopeptidase-like protein remodels gating charge

dynamics in Kv4.2 channels. *J. Gen. Physiol.* 128, 745–753.

Dougherty, K., Santiago-Castillo, J. A., and Covarrubias, M. (2008). Gating charge immobilization in Kv4.2 channels: the basis of closed-state inactivation. *J. Gen. Physiol.* 131, 257–273.

Eberwine, J. (2001). Single-cell molecular biology. *Nat. Neurosci.* 4(Suppl), 1155–1156.

Engel, J., Rabba, J., and Schild, D. (1996). A transient, RCK4-like K^+ current in cultured Xenopus olfactory bulb neurons. *Pflugers Arch.* 432, 845–852.

Everill, B., Rizzo, M. A., and Kocsis, J. D. (1998). Morphologically identified cutaneous afferent DRG neurons express three different potassium currents in varying proportions. *J. Neurophysiol.* 79, 1814–1824.

Fang, X., Djouhri, L., McMullan, S., Berry, C., Waxman, S. G., Okuse, K., and Lawson, S. N. (2006). Intense isolectin-B4 binding in rat dorsal root ganglion neurons distinguishes C-fiber nociceptors with broad action potentials and high Nav1.9 expression. *J. Neurosci.* 26, 7281–7292.

Gold, M. S., Shuster, M. J., and Levine, J. D. (1996). Characterization of six voltage-gated K^+ currents in adult rat sensory neurons. *J. Neurophysiol.* 75, 2629–2646.

Gutman, G. A., Chandy, K. G., Adelman, J. P., Aiyar, J., Bayliss D. A., Clapham, D. E., Covarrubias, M., Desir, G. V., Furuichi, K., Ganetzky, B., Garcia, M. L., Grissmer, S., Jan, L. Y., Karschin, A., Kim, D., Kuperschmidt, S., Kurachi, Y., Lazdunski, M., Lesage, F., Lester, H. A., McKinnon, D., Nichols, C. G., O'Kelly, I., Robbins, J., Robertson, G. A., Rudy, B., Sanguinetti, M., Seino, S., Stuehmer, W., Tamkun, M. M., Vandenberg, C. A., Wei, A., Wulff, H., and Wymore, R. S. (2003). International Union of Pharmacology. XLI. Compendium of voltage-gated ion channels: potassium channels. *Pharmacol. Rev.* 55, 583–586.

Hamill, O. P., Marty, A., Neher, E., Sakmann, B., and Sigworth, F. J. (1981). Improved patch-clamp techniques for high-resolution current recording from cells and cell-free membrane patches. *Pflugers Arch.* 391, 85–100.

Hoffman, D. A., Magee, J. C., Colbert, C. M., and Johnston, D. (1997). K^+ channel regulation of signal propagation in dendrites of hippocampal pyramidal neurons. *Nature* 387, 869–875.

Holmqvist, M. H., Cao, J., Hernandez-Pineda, R., Jacobson, M. D., Carroll, K. I., Sung, M. A., Betty, M., Ge P., Gilbride, K. J., Brown, M. E., Jurman, M. E., Lawson, D., Silos-Santiago, I., Xie, Y., Covarrubias, M., Rhodes, K. J., Distefano, P. S., and An, W. F. (2002). Elimination of fast inactivation in Kv4 A-type potassium channels by an auxiliary subunit domain. *Proc. Natl. Acad. Sci. U.S.A.* 99, 1035–1040.

Huang, H. Y., Cheng, J. K., Shih, Y. H., Chen, P. H., Wang, C. L., and Tsaur, M. L. (2005). Expression of A-type K^+ channel alpha subunits Kv 4.2 and Kv 4.3 in rat spinal lamina II excitatory interneurons and colocalization with pain-modulating molecules. *Eur. J. Neurosci.* 22, 1149–1157.

Huang, H. Y., Liao, C. W., Chen, P. H., and Tsaur, M. L. (2006). Transient expression of A-type K^+ channel alpha subunits Kv4.2 and Kv4.3 in rat spinal neurons during development. *Eur. J. Neurosci.* 23, 1142–1150.

Jackson, A. C., and Bean, B. P. (2007). State-dependent enhancement of subthreshold A-type potassium current by 4-aminopyridine in tuberomammillary nucleus neurons. *J. Neurosci.* 27, 10785–10796.

Jerng, H. H., and Covarrubias, M. (1997). K^+ channel inactivation mediated by the concerted action of the cytoplasmic N- and C-terminal domains. *Biophys. J.* 72, 163–174.

Jerng, H. H., Pfaffinger, P. J., and Covarrubias M. (2004). Molecular physiology and modulation of somatodendritic A-type potassium channels. *Mol. Cell Neurosci.* 27, 343–369.

Johnston, D., Christie, B. R., Frick, A., Gray, R., Hoffman, D. A., Schexnayder, L. K., Watanabe, S., and Yuan, L. L. (2003). Active dendrites, potassium channels and synaptic plasticity. *Philos. Trans. R. Soc. Lond., B, Biol. Sci.* 358, 667–674.

Kaulin, Y. A., Santiago-Castillo, J. A., Rocha, C. A., and Covarrubias, M. (2008). Mechanism of the modulation of Kv4:KChIP-1 channels by external K^+. *Biophys. J.* 94, 1241–1251.

Khaliq, Z. M., and Bean, B. P. (2008). Dynamic, nonlinear feedback regulation of slow pacemaking by A-type potassium current in ventral tegmental area neurons. *J. Neurosci.* 28, 10905–10917.

Kim, D. S., Choi, J. O., Rim, H. D., and Cho, H. J. (2002). Downregulation of voltage-gated potassium channel alpha gene expression in dorsal root ganglia following chronic constriction injury of the rat sciatic nerve. *Brain Res. Mol. Brain Res.* 105, 146–152.

Kim, J., Wei, D. S., and Hoffman, D. A. (2005). Kv4 potassium channel subunits control action potential repolarization and frequency dependent broadening in hippocampal CA1 pyramidal neurons. *J. Physiol.* 569, 41–57.

Korngreen, A., Kaiser, K. M., and Zilberter, Y. (2005). Subthreshold inactivation of voltage-gated K^+ channels modulates action potentials in neocortical bitufted interneurones from rats. *J. Physiol.* 562, 421–437.

Kostyuk, P. G., Veselovsky, N. S., Fedulova, S. A., and Tsyndrenko, A. Y. (1981). Ionic currents in the somatic membrane of rat dorsal root ganglion neurons-III. Potassium currents. *Neuroscience* 6, 2439–2444.

Lange, K., Sinsheimer, J. S., and Sobel, E. (2005). Association testing with Mendel. *Genet. Epidemiol.* 29, 36–50.

Li, M., Jan, Y. N., and Jan, L. Y. (1992). Specification of subunit assembly by the hydrophilic amino-terminal domain of the Shaker potassium channel. *Science* 257, 1225–1230.

Liss, B., Franz, O., Sewing, S., Bruns, R., Neuhoff, H., and Roeper, J. (2001). Tuning pacemaker frequency of individual dopaminergic neurons by Kv4.3L and KChip3.1 transcription. *EMBO J.* 20, 5715–5724.

Malin, S. A., and Nerbonne, J. M. (2000). Elimination of the fast transient in superior cervical ganglion neurons with expression of Kv4.2-W362F: molecular dissection of I_A. *J. Neurosci.* 20, 5191–5199.

Malin, S. A., and Nerbonne, J. M. (2001). Molecular heterogeneity of the voltage-gated fast transient outward K^+ current, I_{Af}, in mammalian neurons. *J. Neurosci.* 21, 8004–8014.

Nerbonne, J. M., and Guo, W. (2002). Heterogeneous expression of voltage-gated potassium channels in the heart: roles in normal excitation and arrhythmias. *J. Cardiovasc. Electrophysiol.* 13, 406–409.

Pak, M. D., Baker, K., Covarrubias, M., Butler, A., Ratcliffe, A., and Salkoff, L. (1991). mShal, a subfamily of A-type K^+ channel cloned from mammalian brain. *Proc. Natl. Acad. Sci. U.S.A.* 88, 4386–4390.

Petersen, K. R., and Nerbonne, J. M. (1999). Expression environment determines K^+ current properties: Kv1 and Kv4 alpha-subunit-induced K^+ currents in mammalian cell lines and cardiac myocytes. *Pflugers Arch.* 437, 381–392.

Rasband, M. N., Park, E. W., Vanderah, T. W., Lai, J., Porreca, F., and Trimmer, J. S. (2001). Distinct potassium channels on pain-sensing neurons. *Proc. Natl. Acad. Sci. U.S.A.* 98, 13373–13378.

Rettig, J., Heinemann, S. H., Wunder, F., Lorra, C., Parcej, D. N., Dolly, J. O., and Pongs, O. (1994). Inactivation properties of voltage-gated K^+ channels altered by presence of beta-subunit. *Nature* 369, 289–294.

Roeper, J., Lorra, C., and Pongs, O. (1997). Frequency-dependent inactivation of mammalian A-type K^+ channel Kv1.4 regulated by Ca^{2+}/calmodulin-dependent protein kinase. *J. Neurosci.* 17, 3379–3391.

Rozen, S., and Skaletsky, H. (2000). Primer3 on the WWW for general users and for biologist programmers. *Methods Mol. Biol.* 132, 365–386.

Safronov, B. V., Bischoff, U., and Vogel, W. (1996). Single voltage-gated K^+ channels and their functions in small dorsal root ganglion neurones of rat. *J. Physiol.* 493(Pt 2), 393–408.

Salkoff, L., Baker, K., Butler, A., Covarrubias, M., Pak, M. D., and Wei, A. (1992). An essential 'set' of K^+ channels conserved in flies, mice and humans. *Trends Neurosci.* 15, 161–166.

Scott, S. A. (1992). Sensory Neurons: Diversity, Development and Plasticity. New York, Oxford University Press.

Sculptoreanu, A., Yoshimura, N., and de Groat, W. C. (2004). KW-7158 [(2S)-(+)-3,3,3-trifluoro-2-hydroxy-2-methyl-N-(5,5,10-trioxo-4,10-dihydro thieno[3,2-c][1]benzothiepin-9-yl)propanamide] enhances A-type K^+ currents in neurons of the dorsal root ganglion of the adult rat. *J. Pharmacol. Exp. Ther.* 310, 159–168.

Serodio, P., and Rudy, B. (1998). Differential expression of Kv4 K^+ channel subunits mediating subthreshold transient K^+ (A-type) currents in rat brain. *J. Neurophysiol.* 79, 1081–1091.

Sheng, M., Tsaur, M. L., Jan, Y. N., and Jan, L. Y. (1992). Subcellular segregation of two A-type K^+ channel proteins in rat central neurons. *Neuron* 9, 271–284.

Shibata, R., Nakahira, K., Shibasaki, K., Wakazono, Y., Imoto, K., and Ikenaka, K. (2000). A-type K^+ current mediated by the Kv4 channel regulates the generation of action potential in developing cerebellar granule cells. *J. Neurosci.* 20, 4145–4155.

Song, W. J., Tkatch, T., Baranauskas, G., Ichinohe, N., Kitai, S. T., and Surmeier, D. J. (1998). Somatodendritic depolarization-activated potassium currents in rat neostriatal cholinergic interneurons are predominantly of the A-type and attributable to coexpression of Kv4.2 and Kv4.1 subunits. *J. Neurosci.* 18, 3124–3137.

Stucky, C. L., and Lewin, G. R. (1999). Isolectin B(4)-positive and -negative nociceptors are functionally distinct. *J. Neurosci.* 19, 6497–6505.

Tan, Z. Y., Donnelly, D. F., and LaMotte, R. H. (2006). Effects of a

chronic compression of the dorsal root ganglion on voltage-gated Na^+ and K^+ currents in cutaneous afferent neurons. *J. Neurophysiol.* 95, 1115–1123.

Vega-Saenz, D. M., Moreno, H., Fruhling, D., Kentros, C., and Rudy, B. (1992). Cloning of ShIII (Shaw-like) cDNAs encoding a novel high-voltage-activating, TEA-sensitive, type-A K^+ channel. *Proc. R. Soc. Lond., B, Biol. Sci.* 248, 9–18.

Vydyanathan, A., Wu, Z. Z., Chen, S. R., and Pan, H. L. (2005). A-type voltage-gated K^+ currents influence firing properties of isolectin B4-positive but not isolectin B4-negative primary sensory neurons. *J. Neurophysiol.* 93, 3401–3409.

Winkelman, D. L., Beck, C. L., Ypey, D. L., and O'Leary, M. E. (2005). Inhibition of the A-type K^+ channels of dorsal root ganglion neurons by the long-duration anesthetic butamben. *J. Pharmacol. Exp. Ther.* 314, 1177–1186.

Wong, M. L., and Medrano, J. F. (2005). Real-time PCR for mRNA quantitation. *Biotechniques* 39, 75–85.

Yuan, W., Burkhalter, A., and Nerbonne, J. M. (2005). Functional role of the fast transient outward K^+ current I_A in pyramidal neurons in (rat) primary visual cortex. *J. Neurosci.* 25, 9185–9194.

Conflict of Interest Statement: The authors declare that the research was conducted in the absence of any commercial or financial relationships that could be construed as a potential conflict of interest.

Received: 25 April 2009; paper pending published: 18 May 2009; accepted: 08 June 2009; published online: 07 July 2009.

*Citation: Na Phuket TR and Covarrubias M (2009) Kv4 channels underlie the subthreshold-operating A-type K^+-current in nociceptive dorsal root ganglion neurons. Front. Mol. Neurosci. (2009) **2**:3. doi:10.3389/neuro.02.003.2009*